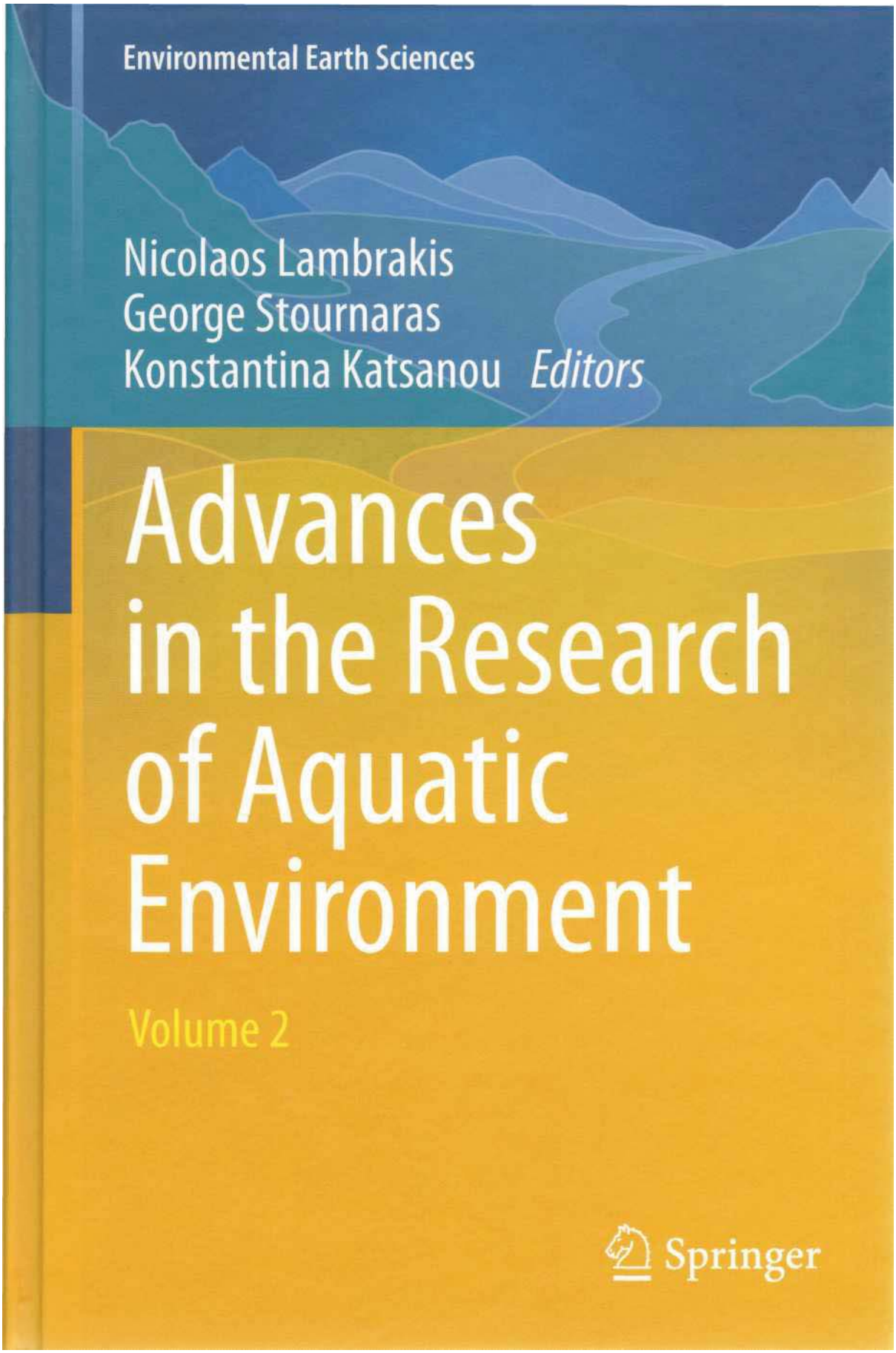
Environmental Earth Sciences
Nicolaos Lambrakis
George Stournaras
Konstantina Katsanou Editors
Advances in the Research of Aquatic Environment
Volume 2
Springer

Adumbration of Amvrakia's spring water pathways, based on detailed geophysical data (Kastraki - Meteora)

J.D. Alexopoulos, S. Dilalos, E. Vassilakis

Faculty of Geology and Geoenvironment, National and Kapodistrian University of Athens, Panepistimiopolis, GR 157 84, Greece. jalexopoulos@geol.uoa.gr

Abstract The Amvrakia spring is located at the bottom of Meteora pillars and more specifically near the village of Kastraki (Kalambaka municipality). It is a seasonal spring since it functions only during the wet period. The Meteora conglomerates which dominate the area are characterized by large discontinuities creating a network of groundwater pathways above the impermeable strata of the underlying marls. The research targets was to define these water pathways in order to understand the mechanism of Amvrakia spring, by mapping the exposed discontinuity network and define their underground extension with the contribution of geophysical techniques. Electrical Resistivity Tomography (ERT) and Very Low Frequency (VLF) methodologies were applied. The VLF method is indicated for the detection of water-bearing fracture zones, but before the application of their filters they had to be processed for topographic corrections, as the area had not smooth relief. Five (5) VLF profiles were conducted with different directions around the spring's area, in order to detect possible conductive zones in the conglomerates surrounding the study area. Moreover, two (2) ERT sections of a total length of 140m were carried out, parallel to existent VLF sections, for cross-checking the geophysical information. Both techniques revealed important conductive zones (<200 Ohm.m) from the south-eastern Meteora conglomerate pillars, possibly interpreted as discontinuities filled with water feeding the spring.

1 Introduction

The Amvrakia spring is located at the Meteora pillars area and more specifically SE of the Kastraki village. The local cultural association was planning to take advantage of the spring and use the water by drilling it. Due to the fact that during the summer the spring suspends its function, they wanted to define its water capacity and mechanism. The study area is surrounded by vertical bluffs consisted of the Meteora conglomerates (Fig. 1) and several difficulties had to be overcome for applying geophysical techniques. The dense vegetation, the increased arduous ac-

N. Lambrakis et al. (Eds.), *Advances in the Research of Aquatic Environment, Vol. 2*
DOI 10.1007/978-3-642-24076-8,

cessibility and the relatively intense relief were the most significant problems that needed to be solved at the fieldwork. Taking into account that the spring's supplying mechanism would be probably through the discontinuities of the conglomerates, we had to define the orientation of these water pathways and the geophysical investigation had to be focused on the detection of conductive zones. Geoelectrical and VLF electromagnetic methods are the most indicative geophysical techniques for such environments (Sharma and Baranwal 2005; Papadopoulos et al. 2008, 2010).

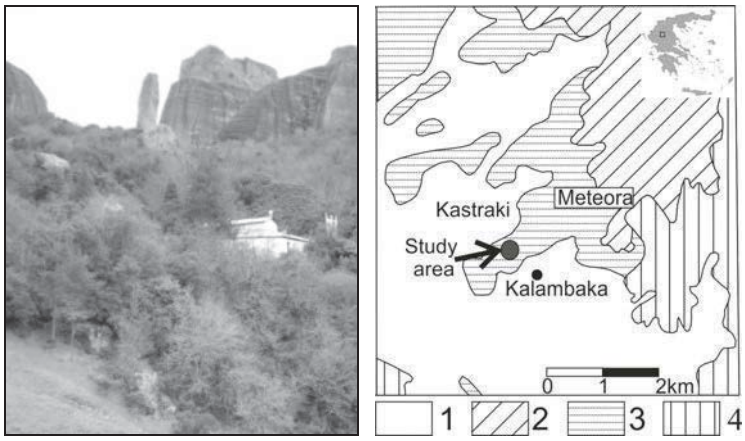

Fig. 1. Schematic geological map of the study area (modified by J.Ferriere et al 2004). 1: Quaternary and recent deposits, 2: Upper Conglomerates (Tsotyli formation), 3: Lower Meteora conglomerates (Pentalofos formation), 4: Oligocene conglomerates, sandstones and marls (Eptachorion formation).

2 Geological and hydrogeological setting

Meteora bluffs belong to the southern part of the Meso-Hellenic molassic basin, of Oligo-Miocene age, consisting mainly of the Meteora conglomerates (Ori and Roveri 1987). The same authors mention that the Meso-Hellenic basin is consisted of Gilbert-type delta deposits and deep channel fills, describing in detail the geometry of the sedimentary bodies of Meteora conglomerate, built by transferred pebbles probably due to the erosion of the Pentalofos unit (Brunn 1956; Ferriere et al. 2004).

More thoroughly, in the area of Meteora bluffs, three of the five units of the Meso-Hellenic molassic basin can be identified (Brunn 1956, Ferriere et al. 2004), while the stratigraphy of the study area is comprised of 3 different formations.

- The deepest formation is part of the transgressive succession of Eptachorion unit consisting of impermeable grey-blue marls of Upper Oligocene age (600 m. thickness).
- Above these marls, massive conglomerate (700 m. thickness) appears normally overlying (Brunn 1956, Papanikolaou et al. 1988), consisting of pebbles up to 20cm in diameter and originated from ophiolithes, marbles, limestones and metamorphic rocks in a sandy matrix. These massive crossed layered conglomerates have been deposited during Aquitaine (Brunn 1956) and are considered to be the southern extension of Pentalofos unit (which can be found north of the study area). It is the material that the impressive pillars are comprised of and, is known as the Meteora conglomerate strata dipping gently westwards (Ori and Roveri 1987). The uppermost part of the formation consists of well-bedded sandstones (Ori and Roveri 1987).
- The upper formation of the area consists of disorganized conglomerates (100 m. thickness) and covers through an angular unconformity the Meteora conglomerate. It is quite often found at the tops of the pillars and seems to be part of Tsotyli unit with Burdigalian age, known as the Upper Conglomerate of Meteora area (Ori and Roveri 1987).

The observed discontinuities (Brunn 1956; Savoyat et al. 1972; Ferriere et al. 2004, this study) in the area have been created after several episodes of the paleogeographic Meso-Hellenic molassic basin evolution, during Upper Eocene-Lower Miocene and their hydrogeological significance is that they usually allow the water flow. The general trending orientation of these almost vertical and open discontinuities is between N040E and N080E. The underlying marls of Eptachorion unit restrict the water flow within the discontinuities of the overlying conglomerates because of their impermeable character.

3 Electromagnetic Survey (VLF)

VLF measurements are proved to be ideal for detecting possible vertical to subvertical conductive zones or karstic structures for hydrogeological investigations (Monteiro Santos 2006; Papadopoulos et al. 2008; Sharma and Baranwal 2005; Dilalos 2009). Based on that and taking into account the tectonic analysis and orientation of the exposed fractures, five (5) profiles were conducted (Fig. 2) with several directions around the spring's area, in order to detect the conductive zones in the conglomerates surrounding the study area. The spacing of the measurement stations was 2 meters, as a more detailed investigation needed to be carried out.

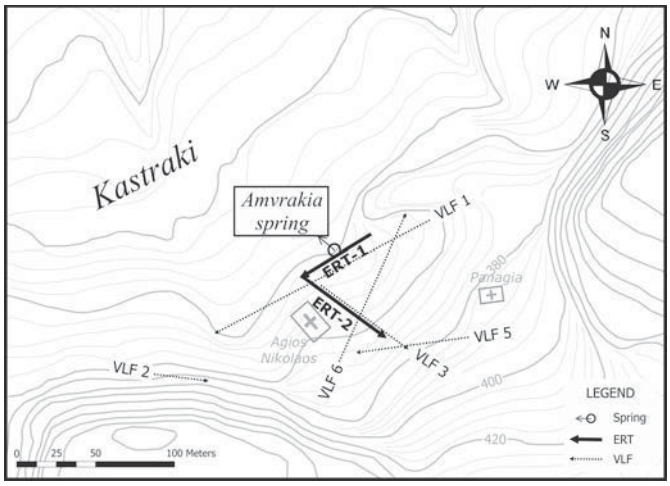

Fig. 2. Topographic sketch map with the ERT and the VLF geophysical sections.

A main VLF source frequency of 23.4 KHz was used, due to the good signal and alignment, towards the direction of the expected anomalies (westwards inclination). The processing of the VLF profiles included smoothing of the raw data and topographic corrections, according to Baker and Myers (1980) and Eberle (1981).

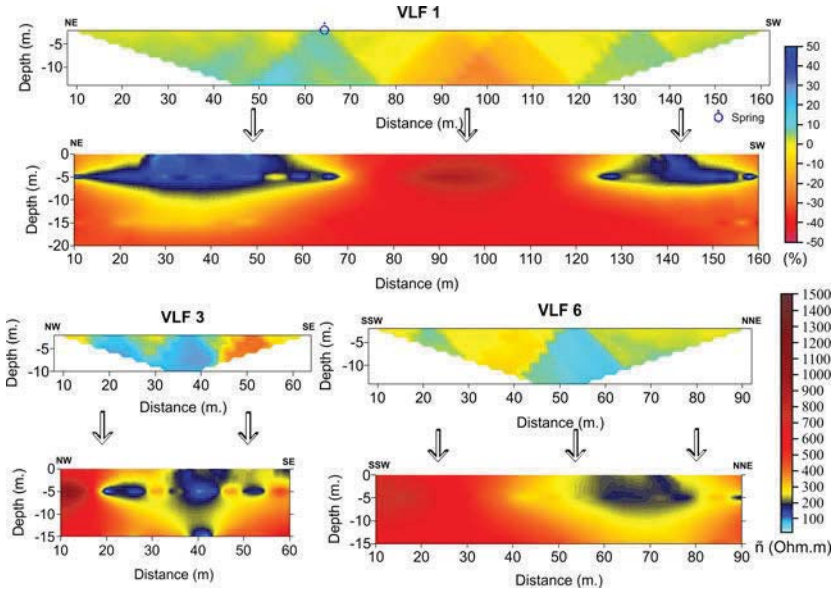

Fig. 3. VLF processing results. The Karous-Hjelt pseudo-sections of profiles VLF 1, VLF 3 and VLF 6 are illustrated. The respective resistivity section derived from inversion with Inv2DVLF software is also included (Initial resistivity 500 Ohm.m with 20 iterations. $RMS_{VLF\ 1}$ =1.16%, $RMS_{VLF\ 3}$=1.82%, $RMS_{VLF\ 6}$=0.95%). Frequency: 23.4 KHz.

Afterwards, we applied the Fraser (1969) and Karous-Hjelt (1979, 1983) filters, which both spotlight the anomalies. Karous-Hjelt filter is providing information of relative current's density distribution with depth, producing the pseudo-sections of Figure 3 (semi-quantity interpretation). In VLF 1 pseudo-section, a main conductive zone is located between 30-75m, after the starting point, probably due to the spring (located at 65m) and a smaller one at 125-140m. VLF 3 pseudo-section indicates a conductive zone at 25-55m, while VLF 6 pseudo-section indicates a main conductive zone between 40-70m and a smaller one at 15-30m.

Additionally, the VLF measurements were processed with *Inv2DVLF* inversion software presented by Monteiro Santos (2006, 2007). The software is basically an algorithm inverting regularized VLF data with the method of smoothed least-squares, based on the scalar tipper originated from the relation of vertical and horizontal component of the magnetic field. The result of this procedure is the subsurface distribution of the resistivity and has been proved to give reliable results similar with those of detailed geoelectrical measurements (Monteiro Santos 2006a and 2006b, Dilalos 2009). The resistivity profiles originating from this procedure, are illustrated in Figure 3 below each Karous-Hjelt pseudo-section, illustrating almost the same conductive (<200 Ohm.m) zones, highlighted due to the color scale. The initial resistivity chosen for the inversion (20 iterations according to the software's author) was 500 Ohm.m, based on the dominant resistivity of the conglomerates (Alexopoulos et al. 2005).

4 Electrical Resistivity Tomography

The ERT technique had been performed in order to validate the conductive zones, detected from VLF measurements in high detail. With this procedure, we investigated the lateral and vertical resistivity distribution.

In the study area, two (2) ERT sections with crossed directions were carried out (Fig. 2), with a total length of 140m. These were both parallel to previously performed VLF sections (VLF 1 and VLF 3), in order to combine results of both geophysical methods. A 41-electrode system providing Wenner array (190 measurement points of apparent resistivity) with electrode spacing up to 2m was applied, along with topographic leveling measurements. The ERT measurements were processed with the *RES2DINV* software of *GeoTomo*. Except for the raw resistivity data, topographic measurements of each section were provided into the software due to the relatively intense relief of the study area. The inverse 2D model resistivity sections, derived from this interpretation are illustrated in Figure 4.

The processing results are quite impressive and detailed. In ERT-1, a conductive (<200 Ohm.m) curvy area has been revealed in the center of the section (15-35m), underneath the spring (overflow mechanism). Another conductive zone (smaller) seems to have been investigated at the distance of 45m. In ERT-2, two parallel conductive zones (<200 Ohm.m) have been investigated, with a clear tilt

to NW, towards the spring. These could be interpreted as water-bearing discontinuities of the conglomerates.

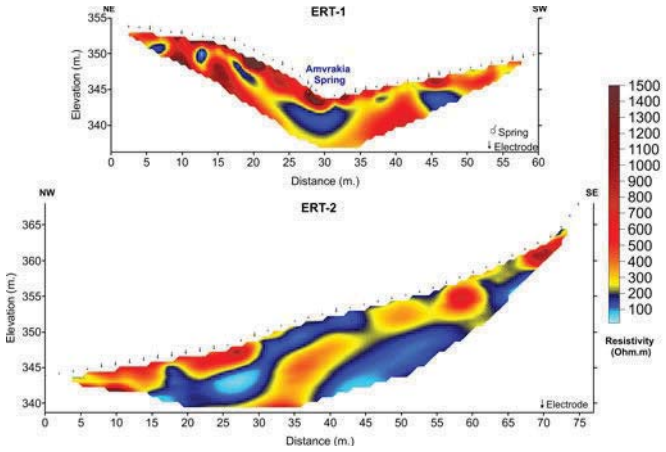

Fig. 4. Electrical Resistivity Tomographies, including topographic relief (ERT-1: 10th iteration, RMS: 2.38%, ERT-2: 11th iteration, RMS: 2.74%).

5 Discussion

Both the geophysical techniques applied in the study area, indicated conductive zones, which was the target of this study. In the two places where we had ERT and VLF sections together, we can also see that the detection of the conductive zones is identical, confirming the results.

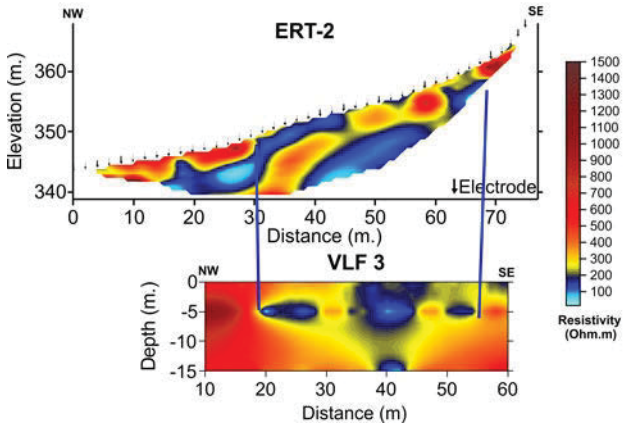

Fig. 5. Comparison of resistivity sections originated from the inversion of the ERT-2 data (up) and from the VLF-3 data inversion with Inv2DVLF (down).

Figure 5 illustrates the resistivity section originated from the inversion of the ERT-2 data (upper Fig. 4), compared with the resistivity section originated from the VLF-3 data inversion with *Inv2DVLF* (down Fig. 4). The ERT section, obviously illustrates the conductive zones in more detail than the VLF measurements.

6 Conclusions

Considering the geology of the area and that the massive conglomerates of the area are resistant (>500 Ohm.m) formations (Alexopoulos et al. 2005), we were able to identify these conductive zones as the most probable water-bearing discontinuities, trending towards the Amvrakia spring. ERT-2 indicates a tilt of these underground pathways to NW (better shown on ERT section), where the spring is located, while the section of ERT-1 indicates a local concavity, which is in agreement with the mechanism of an overflow spring.

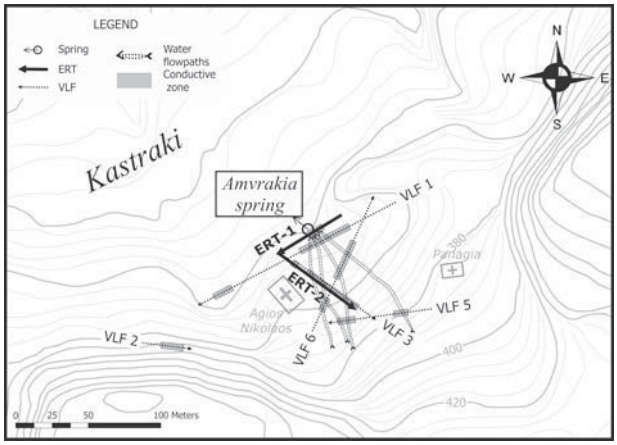

Fig. 6. The investigated conductive zones are being illustrated together with the feeding pathways of the Amvrakia spring.

In Figure 6, all the conductive zones are illustrated along with the delineated water pathways leading towards the spring, corresponding to the discontinuities of the south-eastern Meteora conglomerate pillars arising impressively above the survey area. We have to point out that the spring's water should not be potable, since these adumbrated water pathways run nearby the small cemetery of the neighboring abandoned Agios Nikolaos church.

Acknowledgments The authors would like to thank Prof. A. Kelepertzis for his advices and Mr. A. Chormovas, president of the Kastraki Cultural Association for his support and hospitality. Moreover, we would like to thank Professor Fernardo Monteiro Santos for the kind provision of the *Inv2DVLF* software.

References

Alexopoulos JD, Papadopoulos T, Mastroyannis A (2005) Investigation of hydrogeological factors affecting the potable water wells of Kalampaka urban by using geophysical techniques. Proc. of the 7th Hellenic hydrogeological conference, 19-30

Baker HA, Myers JO (1980) A topographic correction for the VLF-EM profiles based on model studies Geoexploration 18, 135-144

Brunn JH (1956) Etude geologique du Pinde septentrional de la Macedoine occidentale Ann. Geol. Pays. Hellen. 7, 1-358

Dilalos S (2009) Exploration of hydrogeological and environmental conditions with geophysical techniques, at selected sites in Chios island (Greece) M.Sc Thesis. National and Kapodistrian University of Athens, Faculty of Geology and Geoenvironment. Athens

Eberle D (1981) A method of reducing terrain relief effects from VLF-EM data Geoexploration 19, 103-114

Ferriere J, Reynaud J, Pavlopoulos A, Bonneau M, Migiros G, Chanier F, Proust J and Gradin S (2004) Bull. Soc. Geol. Fr. 175/4, 361-381

Fraser D.C. (1969) Contouring of VLF-EM data Geophysics 34/6, 958-967

Karous M (1979) Effect of relief in EM methods with very distant source Geoexploration 17, 33-42

Karous M, Hjelt SE (1983) Linear filtering of VLF dip-angle measurements Geophysical Prospecting 31, 782-794

Monteiro Santos FA (2006) Instructions for running PrepVLF and Inv2DVLF; 2-D inversion of VLF-EM single frequency programs Version 1.0. Lisboa

Monteiro Santos FA (2007) New features PrepVLF and Inv2DVLF, Version 1.1. Lisboa

Monteiro Santos FA, Almeida EP, Gomes M, Pina A (2006) Hydrogeological investigation in Santiago Island (Cabo Verde) using magnetotellurics and VLF methods Journal of African Earth Sciences 45, 421-430

Monteiro Santos FA, Mateus A, Figueiras J, Concalves MA (2006) Mapping groundwater contamination around a landfill facility using the VLF-EM method - A case study Journal of Applied Geophysics 60, 115-125

Ori GG, Roveri M (1987) Geometries of Gilbert-type deltas and large channels in the Meteora Conglomerate, Meso-Hellenic basin (Oligo-Miocene), central Greece. Sedimentology 34, 845-859

Papadopoulos TD, Alexopoulos JD, Dilalos S, Pippidis MJ (2008) Resistivity and VLF measurements for spring mechanism determination at NE Chios Isl. Proc. of the 8th International hydrogeological congress of Greece, 337-346

Papadopoulos TD, Stournaras G, Alexopoulos JD (2010) Geophysical investigations for aquifer detection in fissured rocks of volcanic origin. A case history. Journal of the Balkan Geophysical Society 13/2, 1-8

Papanikolaou DJ, Lekkas EL, Mariolakos ID, Mirkou RM (1988) Contribution to the geodynamic evolution of the Mesohellenic basin (in Greek) Bull. Geol. Soc. Greece 20, 17-36

Sharma SP, Baranwal VC (2005) Delineation of groundwater-bearing fracture zones in a hard rock area integrating very low frequency electromagnetic and resistivity data. Journal of Applied Geophysics 57, 155-166

Savoyat E, Lalechos N, Philippakis N, Bizon G (1972) Geological map of Greece, scale 1:50.000, Kalambaka Sheet. Inst Geol and Miner. Explor., Athens